研究成果の刊行に関する一覧表

書籍

著者氏名	論文タイトル名	書籍全体の編集者名	書　籍　名	出版社名	出版地	出版年	ページ
Kanagawa M, Toda T.	Fukutin and Fukuyama congenital muscular dystrophy.	Taniguchi. N, et.al. eds	Glycoscience Lab Manual	Elsevier Japan	Japan	2008	309-312
Ito N, Miyagoe-Suzuki Y.	Neuronal NOS as a regulator of muscle mass.	Yoshinobu Ohira	Muscle Cell Physiology	Osaka University Press	Osaka, Japan	2009	97-107
Saito F, and Matsumura K.	Dystroglycan and neuromuscular diseases: Its diverging role in muscle, nerve and brain.	Paços A and Nogueira S	Neurochemistry: Mollecular aspects, cellular aspects and clinical applications	NOVA Science Publishers, Inc.	New York	2009	195-209
Miyagoe-Suzuki Y, Uezumi A & Shin'ichi Takeda.	Side population (SP) cells and skeletal muscle differentiation.	Tsuchida K& Takeda S	Recent Advances of Skeletal Muscle Differentiation	Research Signpost	Fort P.O., Trivandrum-695 023, Kerala, India	2009	61-78
Endo T, Manya H, Seta N, Guicheney P.	POMGnT1, POMT1, and POMT2 Mutations in Congenital Muscular Dystrophies.	Fukuda, M.	Methods Enzymol., 479	Elsevier	San Diego, USA	2010	343-352

鈴木友子 武田伸一	II. B. 体性幹細胞と組織修復 5. 骨格筋	松島綱治・ 西脇 徹	炎症・再生医学事典	朝倉書店	東京	2009	453-456
戸田達史 佐竹渉	パーキンソン病の発症関連遺伝子多型	鈴木則宏 祖父江元 荒木信夫 宇川義一 川原信隆	Annual Review 神経 2011	中外医学社	東京	2011	260-267
鈴木友子 遠藤玉夫	POMGnT1	小幡裕一 城石俊彦 芹川忠夫 田中啓二 米川博通	生物機能モデルと新しいリソース・リサーチツール	エル・アイ・シー	東京	2011	368-374
鈴木友子 武田伸一	筋ジストロフィーモデルマウス	秋山徹 奥山隆平 河府和義	マウス・ラット疾患モデル活用 ハンドブック	羊土社	東京	2011	378-393

雑誌

発表者氏名	論文タイトル名	発表誌名	巻号	ページ	出版年
Kumazawa R, Tomiyama H, Li Y, Imamichi Y, Funayama M, Yoshino H, Yokochi F, Fukusako T, Takehisa Y, Kashihara K, Kondo T, Elibol B, Bostantjopoulou S, Toda T, Takahashi H, Yoshii F, Mizuno Y, Hattori N.	Mutation analysis of the PINK1 gene in 391 patients with Parkinson's disease.	Arch Neurol	65	802-808	2008
Mizuta I, Tsunoda T, Satake W, Nakabayashi Y, Watanabe M, Takeda A, Hasegawa K, Nakashima K, Yamamoto M, Hattori N, Murata	Calbindin 1, fibroblast growth factor 20, and α-synuclein in sporadic Parkinson's disease.	Hum Genet	124	89-94	2008

M, Toda T.					
Sato S, Omori Y, Katoh K, Kondo M, Kanagawa M, Miyata K, Funabiki K, Koyasu T, Kajimura N, Miyoshi T, Sawai H, Kobayashi K, Tani A, Toda T, Usukura J, Tano Y, Fujikado T, Furukawa T.	Pikachurin, a dystroglycan ligand, is essential for photoreceptor ribbon synapse formation.	Nature Neurosci	11	923-931	2008
Fujikake N, Nagai Y, Popiel HA, Okamoto Y, Yamaguchi M, Toda T.	Heat shock transcription factor 1-activating compounds suppress polyglutamine-induced neurodegeneration through induction of multiple molecular chaperones.	J Biol Chem	283	26188-26197	2008
Wakayama Y, Inoue M, Kojima H, Yamashita S, Shibuya S, Jimi T, Hara H, Matsuzaki Y, Oniki H, Kanagawa M, Kobayashi K, Toda T.	Reduced expression of sarcospan in muscles of Fukuyama congenital muscular dystrophy.	Histol Histopathol	23	1425-1438	2008
Tomiyama H, Mizuta I, Li Y, Funayama M, Yoshino H, Li L, Murata M, Yamamoto M, Kubo SI, Mizuno Y, Toda T, Hattori N.	LRRK2 P755L variant in sporadic Parkinson's disease.	J Hum Genet	53	1012-1015	2008
Ohsawa Y, Okada T, Kuga A, Hayashi S, Murakami T, Tsuchida K, Noji S, Sunada Y.	Caveolin-3 regulates myostatin signaling.	Acta Myol	27	19-24	2008
Kinouchi N, Ohsawa Y, Ishimaru N, Ohuchi H, Sunada Y, Hayashi Y, Tanimoto Y, Moriyama K, Noji	Atelocollagen-mediated local and systemic applications of myostatin-targeting siRNA increase skeletal muscle mass.	Gene Ther	15	1126-1130	2008

S.					
Nishiyama A, Ampong BN, Ohshima S, Shin JH, Nakai H, Imamura M, Miyagoe-Suzuki Y, Okada T, Takeda S.	Recombinant adeno-associated virus type 8-mediated extensive therapeutic gene delivery into skeletal muscle of alpha-sarcoglycan-defici ent mice.	Hum Gene Ther	19	719-730	2008
Tanihata J, Suzuki N, Miyagoe-Suzuki Y, Imaizumi K, Takeda S.	Downstream utrophin enhancer is required for expression of utrophin in skeletal muscle.	J Gene Med	10	702-713	2008
Motohashi N, Uezumi A, Yada E, Fukada S, Fukushima K, Imaizumi K, Miyagoe-Suzuki Y, Takeda S.	Muscle CD31(-) CD45(-) side population cells promote muscle regeneration by stimulating proliferation and migration of myoblasts.	Am J Pathol	173	781-791	2008
Segawa M, Yamamoto Y, Yahagi H, Kanematsu M, Sato M, Ito T, Uezumi A, Hayashi S, Miyagoe-Suzuki Y, Takeda S, Tsujikawa K, Yamamoto H.	Suppression of macrophage functions impairs skeletal muscle regeneration with severe fibrosis.	Exp Cell Res	314	3232-3244	2008
Popiel HA, Nagai Y, Fujikake N, Toda T.	Delivery of the aggregate inhibitor peptide QBP1 into the mouse brain using PTDs and its therapeutic effect on polyglutamine disease mice.	Neurosci Lett	449	87-92	2009
Kanagawa M, Nishimoto A, Chiyonobu T, Takeda S, Miyagoe-Suzuki Y, Wang F, Fujikake N, Taniguchi M, Lu Z, Tachikawa M, Nagai Y, Tashiro F, Miyazaki J, Tajima Y, Takeda S, Endo T, Kobayashi K, Campbell KP, Toda T.	Residual laminin-binding activity and enhanced dystroglycan glycosylation by LARGE in novel model mice to dystroglycanopathy.	Hum Mol Genet	18	621-631	2009

Okamoto Y, Nagai Y, Fujikake N, Popiel HA, Yoshioka T, Toda T, Inui T.	Surface plasmon resonance characterization of specific binding of polyglutamine aggregation inhibitors to the expanded polyglutamine stretch.	Biochem Biophys Res Commun	378	634-639	2009
Tomita K, Popiel HA, Nagai Y, Toda T, Yoshimitsu Y, Ohno H, Oishi S, Fujii N.	Structure-activity relationship study on polyglutamine binding peptide QBP1.	Bioorg Med Chem	17	1259-1263	2009
Mitsui J, Mizuta I, Toyoda A, Ashida R, Takahashi Y, Goto J, Fukuda Y, Date H, Iwata A, Yamamoto M, Hattori N, Murata M, Toda T, Tsuji S.	Mutations for Gaucher disease confer a high susceptibility to Parkinson disease.	Arch Neurol	66	571-576	2009
Shikishima C, Hiraishi K, Yamagata S, Sugimoto Y, Takemura R, Ozaki K, Okada M, Toda T, Ando J.	Is g an entity? A Japanese twin study using syllogisms and intelligence tests.	Intelligence	37	256-267	2009
Saitsu H, Kurosawa K, Kawara H, Eguchi M, Mizuguchi T, Harada N, Kaname T, Kano H, Miyake N, Toda T, Matsumoto N.	Characterization of the complex 7q21.3 rearrangement in a patient with bilateral split-foot malformation and hearing loss.	Am J Med Genet	149A	1224-1230	2009
Xiong H, Wang S, Kobayashi K, Jiang Y, Wang J, Chang X, Yuan Y, Liu J, Toda T, Fukuyama Y, Wu X.	Fukutin gene retrotransposal insertion in a non-Japanese Fukuyama congenital muscular dystrophy (FCMD) patient.	Am J Med Genet	149A	2403-2408	2009
Sidransky E, Nalls MA, Aasly JO, Aharon-Peretz J, Annesi G, Barbosa ER, Bar-Shira A, Berg D, Bras J, Brice A, Chen CM, Clark LN,	Multicenter analysis of glucocerebrosidase mutations in Parkinson's disease.	N Engl J Med	361	1651-1661	2009

Condroyer C, De Marco EV, Dürr A, Eblan MJ, Fahn S, Farrer MJ, Fung HC, Gan-Or Z, Gasser T, Gershoni-Baruch R, Giladi N, Griffith A, Gurevich T, Januario C, Kropp P, Lang AE, Lee-Chen GJ, Lesage S, Marder K, Mata IF, Mirelman A, Mitsui J, Mizuta I, Nicoletti G, Oliveira C, Ottman R, Orr-Urtreger A, Pereira LV, Quattrone A, Rogaeva E, Rolfs A, Rosenbaum H, Rozenberg R, Samii A, Samaddar T, Schulte C, Sharma M, Singleton A, Spitz M, Tan EK, Tayebi N, Toda T, Troiano AR, Tsuji S, Wittstock M, Wolfsberg TG, Wu YR, Zabetian CP, Zhao Y, Ziegler SG.					
Satake W, Nakabayashi Y, Mizuta I, Hirota Y, Ito C, Kubo M, Kawaguchi T, Tsunoda T, Watanabe M, Takeda A, Tomiyama H, Nakashima K, Hasegawa K, Obata F, Yoshikawa T, Kawakami H, Sakoda S, Yamamoto M, Hattori N, Murata M, Nakamura Y, Toda T.	Genome-wide association study identifies common variants at four loci as genetic risk factors for Parkinson's disease.	Nature Genet	41	1303-1307	2009

Miyagoe-Suzuki Y, Masubuchi N, Miyamoto K, Wada MR, Yuasa S, Saito F, Matsumura K, Kanesaki H, Kudo A, Manya H, Endo T, Takeda S.	Reduced proliferative activity of primary POMGnT1-null myoblasts in vitro.	Mech Dev	126	107-116	2009
Tsuchida K, Nakatani M, Hitachi K, Uezumi A,Sunada Y, Ageta H, Inokuchi K.	Activin signaling as an emerging target for therapeutic interventions.	Cell Commun. Signal	7	15	2009
Chang H, Yoshimoto M, Umeda K, Iwasa T, Mizuno Y, Fukada S, Yamamoto H, Motohashi N, Miyagoe-Suzuki Y, Takeda S, Heike T, Nakahata T.	Generation of transplantable, functional satellite-like cells from mouse embryonic stem cells.	FASEB J.	23	1907-1919	2009
Kogo H, Kowa H, Yamada K, Bolor H, Tsutsumi M, Ohye T, Inagaki H, Taniguchi M, Toda T, Kurahashi K.	Screening of genes involved in chromosome segregation during meiosis I: towards the identification of genes responsible for infertility in humans.	J Hum Genet	55	293-299	2010
Tan EK, Kwok HH, Tan LC, Zhao WT, Prakash KM, Au WL, Pavanni R, Ng YY, Satake W, Zhao Y, Toda T, Liu JJ.	Analysis of GWAS-linked loci in Parkinson disease reaffirms PARK16 as a susceptibility locus.	Neurology	75	508-512	2010
Kanagawa M, Omori Y, Sato S, Kobayashi K, Miyagoe-Suzuki Y, Takeda S, Endo T, Furukawa T, Toda T.	Post-translational maturation of dystroglycan is necessary for pikachurin binding and ribbon synaptic localization.	J Biol Chem	285	31208-31216	2010
Manya H., Akasaka-Manya K., Nakajima A., Kawakita M.,	Role of *N*-glycans in maintaining the activity of protein *O*-mannosyltransferases	J. Biochem.	147	337-344	2010

Endo T.	POMT1 and POMT2.				
Avşar-Ban E, Ishikawa H, Manya H, Watanabe M, Akiyama S, Miyake H, Endo T, Tamaru Y.	Protein *O*-mannosylation is necessary for normal embryonic development in zebrafish.	Glycobiology	20	1089-1102	2010
Miyagoe-Suzuki Y, Takeda S.	Gene therapy for muscle disease.	Exp. Cell Res	316	3087-3092	2010
Fukada S, Morikawa D, Yamamoto Y, Yoshida T, Sumie N, Yamaguchi M, Ito T, Miyagoe-Suzuki Y, Takeda S, Tsujikawa K, Yamamoto H.	Genetic background affects properties of satellite cells and mdx phenotypes.	Am. J. Pathol	176	2414-2424	2010
Yajima H, Motohashi N, Ono Y, Sato S, Ikeda K, Masuda S, Yada E, Miyagoe-Suzuki Y, Takeda S, Kawakami K.	Six family genes control the proliferation and differentiation of muscle satellite cells.	Exp. Cell Res	316	2932-2944	2010
Kojima K, Nosaka H, Kishimoto Y, Nishiyama Y, Fukuda S, Shimada M, Kodaka K, Saito F, Matsumura K, Shimizu T, Toda T, Takeda S, Kawachi H, Uchida S.	Defective glycosylation of α-dystroglycan contributes to podocyte flattening.	Kidney Int	79	311-316	2011
Krüger R, Sharma M, Riess O, Gasser T, Van Broeckhoven C, Theuns J, Aasly J, Annesi G, Bentivoglio AR, Brice A, Djarmati A, Elbaz A, Farrer M, Ferrarese C, Gibson JM, Hadjigeorgiou GM, Hattori N, Ioannidis JP, Jasinska-Myga B, Klein C, Lambert JC, Lesage S, Lin	A large-scale genetic association study to evaluate the contribution of Omi/HtrA2 (PARK13) to Parkinson's disease.	Neurobiol Aging	32	548.e9-548.e18.	2011

JJ, Lynch T, Mellick GD, de Nigris F, Opala G, Prigione A, Quattrone A, Ross OA, Satake W, Silburn PA, Tan EK, Toda T, Tomiyama H, Wirdefeldt K, Wszolek Z, Xiromerisiou G, Maraganore DM; for the Genetic Epidemiology of Parkinson's disease consortium.					
Chihara N, Aranami T, Sato W, Miyazaki Y, Miyake S, Okamoto T, Ogawa M, Toda T, Yamamura T.	Interleukin 6 signaling promotes anti-aquaporin 4 autoantibody production from plasmablasts in neuromyelitis optica.	Proc Natl Acad Sci U S A	108	3701-3706	2011
Clarke NF, Maugenre S, Vandebrouck A, Urtizberea JA, Willer T, Peat R, Gray F, Bouchet C, Manya H, Vuillaumier-Barrot S, Endo T, Chouery E, Campbell KP, Mégarbané A, Guicheney P.	Congenital Muscular Dystrophy type 1D (MDC1D) due to a large intragenic insertion/deletion involving intron 10 of the LARGE gene.	Eur. J. Hum. Genet	19	452-457	2011
Nakatani M, Kokubo M, Ohsawa Y,Sunada Y, Tsuchida K.	Follistatin-derived peptide expression in muscle decreases adipose tissue mass and prevents hepatic steatosis.	Am. J. Physiol. Endocrinol. Metab	300	E543-553	2011
Kawakami E, KinouchiN, Adachi T, Ohsawa Y, Ishimaru N, OhuchiH, Sunada Y, HayashiY, Tanaka E, Noji S.	Atelocollagen-mediated systemic administration of myostatin-targeting siRNA improves muscular atrophy in caveolin-3-deficient mice.	Dev Growth Differ	53	48-54	2011
Shimizu N, Yoshikawa N, Ito N, Maruyama T, Suzuki Y, Takeda	Crosstalk between glucocorticoid receptor and nutritional sensor mTOR in skeletal	Cell Metabolism	13	170-182	2011

S, Nakae J, Tagata Y, Nishitani S, Takehana K, Sano M, Fukuda K, Suematsu M, Chikao Morimoto C, Tanaka H.	muscle.				
Sun H, Satake W, Zhang C, Nagai Y, Tian Y, Fu S, Yu J, Qian Y, Qian Y, Chu J, Toda T.	Genetic and clinical analysis in a Chinese parkinsonism-predominant spinocerebellar ataxia type 2 family.	J Hum Genet	In Press		
Saito F, Matsumura K.	Fukuyama-type congenital muscular dystrophy and defective glycosylation of α-dystroglycan.	Skeletal Muscle	In press		
Takahashi H, Kanesaki H, Igarashi T, Kameya S, Yamaki K, Mizota A, Kudo A, Miyagoe-Suzuki Y, Takeda S, Takahashi H.	Reactive gliosis of astrocytes and Muller glial cells in retina of POMGnT1-deficient mice.	Molecular and Cellular Neuroscience	In press		
戸田達史	福山型筋ジストロフィー	ビジュアル疾患解説　眼で見る遺伝病とターナー症候群	2	6-7	2008
戸田達史	孤発性パーキンソン病のゲノムワイドスクリーニング	ゲノム医学	8	105-110	2008
小林千浩 戸田達史	認知と遺伝子	Cognition and Dementia	7	35-43	2008
谷口真理子 戸田達史	筋ジストロフィー	小児内科	40	1308-1314	2008
水田依久子 戸田達史	孤発性パーキンソン病のメカニズム	成人病と生活習慣病	38	887-892	2008
戸田達史	Alzheimer 病と遺伝	成人病と生活習慣病	38	1205-1210	2008
戸田達史	福山型筋ジストロフィーの発見とその類縁疾患における病態	蛋白質　核酸酵素	53	1771-1780	2008
砂田芳秀	抗マイオスタチン療法	医学のあゆみ	226	402-407	2008
水田依久子 戸田達史 澤田誠	家族性パーキンソン病は孤発性パーキンソンのモデルになるか？	Frontiers in Parkinson Disease	2	79-87	2009
戸田達史	パーキンソン病関連遺	最新医学	64	872-879	2009

	伝子の全ゲノム関連解析				
戸田達史	パーキンソン病のゲノムワイド関連解析	細胞	41	198-202	2009
戸田達史	福山型先天性筋ジストロフィー	小児科	50	899-906	2009
戸田達史 佐竹渉 水田依久子	関連遺伝子 疾患感受性遺伝子の同定	日本臨床	67 増刊号 4	83-90	2009
三井純 戸田達史	孤発性パーキンソン病の分子遺伝学	実験医学	27 増刊号 12	1854-1859	2009
戸田達史	パーキンソン病のゲノミックス	老年精神医学雑誌	20	973-979	2009
戸田達史	福山型筋ジストロフィーおよび類縁疾患の病態・治療戦略	臨床神経学	49	859-862	2009
鈴木友子 武田伸一	ゲノムと再生医療「筋ジストロフィーに対する先端治療法の開発」	ゲノム医学	3巻　3号	47-50	2009
戸田達史	筋ジストロフィーの最新検査	SRL 宝函	30(4)	4-11	2010
戸田達史 佐竹渉	孤発性パーキンソン病のリスク遺伝子	最新医学	65	806-813	2010
戸田達史 佐竹渉	ゲノムワイド関連解析によるパーキンソン病リスク遺伝子の同定	医学のあゆみ	233	640-642	2010
戸田達史	パーキンソン病の GWAS	Bio Clinica	25	477-482	2010
戸田達史	福山型筋ジストロフィーの治療戦略	難病と在宅のケア	16	41-43	2010
戸田達史	福山型筋ジストロフィー	JFNMH Newsletter	7	2-6	2010
小田哲也　苅田典生　濱口浩敏 田中恵子　戸田達史	抗 aquaporin-4 抗体陽性症例の治療経験	神経内科	73	194-198	2010
戸田達史	福山型先天性筋ジストロフィーについて	厚生労働科学研究事業 こころの健康科学研究		9-10	2010
戸田達史	疾患感受性遺伝子	Current Therapy	28	859-860	2010
徳田隆彦 戸田達史	パーキンソン病	Clinical Neuroscience	28	1405-1409	2010
佐竹渉 戸田達史	パーキンソン病の遺伝的背景	綜合臨牀	59	2388-2391	2010
佐竹渉 戸田達史	パーキンソン病診療Q&A パーキンソン病の遺伝的リスクについて	Frontiers in Parkinson Disease	4	48-52	2011

野田 佳克　大塚 喜久　安井 直子　関口 兼司　川上 史　中村 栄男　苅田 典生　戸田 達史	脳炎様の画像所見を呈した加齢性Epstein-Barr Virus関連B細胞リンパ増殖性異常症の1例	臨床神経学	51	207-210	2011
砂田芳秀	筋ジストロフィーの分子病態	神経治療学	27	781-784	2010
鈴木友子 武田伸一	特集　再生医療—臨床応用へ向けての現状と課題「筋ジストロフィー」	総合リハビリテーション	39	25-29	2011
斉藤史明 松村喜一郎	α-ジストログリカンの機能異常と筋ジストロフィー	生体の科学	In press		

IV. 研究成果の刊行物・別刷

nature neuroscience

Pikachurin, a dystroglycan ligand, is essential for photoreceptor ribbon synapse formation

Shigeru Sato[1–3], Yoshihiro Omori[1], Kimiko Katoh[1], Mineo Kondo[4], Motoi Kanagawa[5], Kentaro Miyata[4], Kazuo Funabiki[6], Toshiyuki Koyasu[4], Naoko Kajimura[7], Tomomitsu Miyoshi[8], Hajime Sawai[8], Kazuhiro Kobayashi[5], Akiko Tani[1], Tatsushi Toda[5], Jiro Usukura[9], Yasuo Tano[2], Takashi Fujikado[2,3] & Takahisa Furukawa[1]

Exquisitely precise synapse formation is crucial for the mammalian CNS to function correctly. Retinal photoreceptors transfer information to bipolar and horizontal cells at a specialized synapse, the ribbon synapse. We identified pikachurin, an extracellular matrix–like retinal protein, and observed that it localized to the synaptic cleft in the photoreceptor ribbon synapse. *Pikachurin* null-mutant mice showed improper apposition of the bipolar cell dendritic tips to the photoreceptor ribbon synapses, resulting in alterations in synaptic signal transmission and visual function. Pikachurin colocalized with both dystrophin and dystroglycan at the ribbon synapses. Furthermore, we observed direct biochemical interactions between pikachurin and dystroglycan. Together, our results identify pikachurin as a dystroglycan-interacting protein and demonstrate that it has an essential role in the precise interactions between the photoreceptor ribbon synapse and the bipolar dendrites. This may also advance our understanding of the molecular mechanisms underlying the retinal electrophysiological abnormalities observed in muscular dystrophy patients.

The establishment of precise synaptic connections between neurons in the developing and mature CNS is crucial for normal nervous system functions, including perception, memory and cognition. Thus, elucidating the mechanisms by which synapses develop and are modified is a central aim in neurobiology. Over the past few decades, a large number of protein components have been identified that are required for synapse morphogenesis and neurotransmitter release[1,2]. However, the molecules and mechanisms underlying specific synapse connections in the vertebrate CNS are still poorly understood.

The neural retina is developmentally a part of the CNS and is where the first stage of visual signal processing occurs. Visual information is transmitted from photoreceptor cells to the ganglion cells via bipolar interneurons. The photoreceptor axon terminal forms a specialized structure, the ribbon synapse, which specifically connects photoreceptor synaptic terminals with bipolar and horizontal cell terminals in the outer plexiform layer (OPL) of the retina. Although various presynaptic factors that are required for synaptic ribbon structure, such as CtBp2/RIBEYE, piccolo and bassoon, have been identified[3,4], the mechanism of ribbon synapse apposition specific to bipolar and horizontal terminals remains totally unknown.

Mutations in the dystrophin-glycoprotein complex (DGC) cause various forms of muscular dystrophy[5]. Dystroglycan, a central component of the DGC, functions as a cellular receptor that is expressed in a variety of tissues, including the CNS[6]. Dystroglycan precursor protein is cleaved into two subunits, α-dystroglycan and β-dystroglycan[7]. α-dystroglycan is a heavily glycosylated extracellular protein and has the potential to bind to several extracellular proteins containing the laminin-G domain, including laminin-α1, laminin-α2, agrin, perlecan and neurexins[8–11]. The DGC components are also expressed in the retina[12–15]. Altered electroretinograms (ERGs) are frequently found in individuals with Duchenne and Becker muscular dystrophy, indicating that the DGC is necessary for normal retinal physiology[16–18]. However, the functional role of DGC in the retina is elusive.

We isolated and characterized mouse pikachurin, a dystroglycan ligand in the retina. To the best of our knowledge, pikachurin is the first dystroglycan ligand to interact with the presynaptic dystroglycan. Our results demonstrate that pikachurin is critically involved in both the normal photoreceptor ribbon synapse formation and physiological functions of visual perception. This may also shed light on the molecular mechanisms underlying the retinal

[1]Department of Developmental Biology, Osaka Bioscience Institute, 6-2-4 Furuedai, Suita, Osaka, 565-0874, Japan. [2]Department of Ophthalmology, Osaka University Graduate School of Medicine, 2-2 Yamadaoka, Suita, Osaka, 565-0871, Japan. [3]Department of Visual Science, Osaka University Graduate School of Medicine, 2-2 Yamadaoka, Suita, Osaka, 565-0871, Japan. [4]Department of Ophthalmology, Nagoya University Graduate School of Medicine, 65 Tsuruma-cho, Showa-ku, Nagoya, 466-8550, Japan. [5]Division of Clinical Genetics, Department of Medical Genetics, Osaka University Graduate School of Medicine, 2-2 Yamadaoka, Suita, Osaka, 565-0871, Japan. [6]Department of Systems Biology, Osaka Bioscience Institute, 6-2-4 Furuedai, Suita, Osaka, 565-0874, Japan. [7]Research Center for Ultrahigh-Voltage Electron Microscopy, Osaka University, 7-1 Mihogaoka, Ibaraki, Osaka, 567-0047, Japan. [8]Department of Physiology, Osaka University Graduate School of Medicine, 2-2 Yamadaoka, Suita, Osaka, 565-0871, Japan. [9]Department of Materials Physics and Engineering, Nagoya University Graduate School of Engineering, 1-1 Furo-cho, Chikusa-ku, Nagoya, 464-8603, Japan. Correspondence should be addressed to T.F. (furukawa@obi.or.jp).

Received 1 May; accepted 12 June; published online 20 July 2008; doi:10.1038/nn.2160

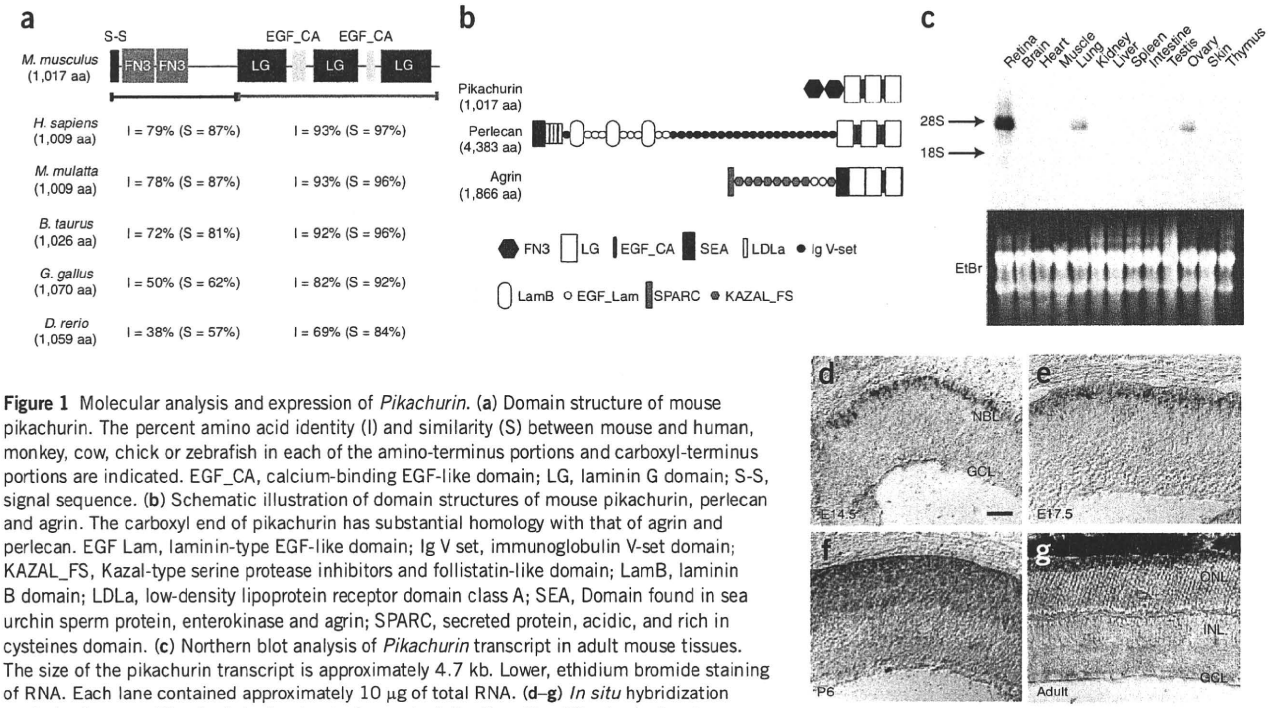

Figure 1 Molecular analysis and expression of *Pikachurin*. (**a**) Domain structure of mouse pikachurin. The percent amino acid identity (I) and similarity (S) between mouse and human, monkey, cow, chick or zebrafish in each of the amino-terminus portions and carboxyl-terminus portions are indicated. EGF_CA, calcium-binding EGF-like domain; LG, laminin G domain; S-S, signal sequence. (**b**) Schematic illustration of domain structures of mouse pikachurin, perlecan and agrin. The carboxyl end of pikachurin has substantial homology with that of agrin and perlecan. EGF Lam, laminin-type EGF-like domain; Ig V set, immunoglobulin V-set domain; KAZAL_FS, Kazal-type serine protease inhibitors and follistatin-like domain; LamB, laminin B domain; LDLa, low-density lipoprotein receptor domain class A; SEA, Domain found in sea urchin sperm protein, enterokinase and agrin; SPARC, secreted protein, acidic, and rich in cysteines domain. (**c**) Northern blot analysis of *Pikachurin* transcript in adult mouse tissues. The size of the pikachurin transcript is approximately 4.7 kb. Lower, ethidium bromide staining of RNA. Each lane contained approximately 10 μg of total RNA. (**d–g**) *In situ* hybridization analysis of mouse *Pikachurin* in the developing and adult retina. The *Pikachurin* signal was detected in the apical side of NBL at E14.5 (**d**) and E17.5 (**e**). P6 (**f**) and adult (**g**) retina had the *Pikachurin* signal in the prospective photoreceptor layer and the photoreceptor layer, respectively. GCL, ganglion cell layer; INL, inner nuclear layer; ONL, outer nuclear layer. Scale bar represents 50 μm.

electrophysiological abnormalities observed in individuals with Duchenne and Becker muscular dystrophy.

RESULTS

Isolation of pikachurin

Otx2 is an important transcription factor for the cell fate determination and development of retinal photoreceptor cells[19,20]. We previously reported that the cell fates of both rod and cone photoreceptors are converted to that of amacrine-like cells in the *Otx2* conditional knockout (CKO) mouse line that was created by mating $Otx2^{flox/flox}$ mice with *Crx-Cre* transgenic mice, which express cre recombinase in developing photoreceptors. We hypothesized that transcripts from various genes, which are important for photoreceptor development, maintenance and function, are relatively downregulated in the *Otx2* CKO retina compared with those of the wild-type retina. To identify genes that regulate photoreceptor development, we carried out a microarray analysis comparing the retinal gene expression profiles of wild-type and *Otx2* CKO mouse retinas (data not shown). In this screen, we identified *Pikachurin*, a gene that encoded a previously unknown extracellular matrix (ECM)-like protein containing laminin G and EGF-like domains (**Fig. 1a**).

To confirm whether or not *Pikachurin* transcription is regulated by Otx2, we carried out an RT-PCR analysis. *Pikachurin* expression was absent in the *Otx2* CKO mice retina (**Supplementary Fig. 1** online), indicating that *Pikachurin* is actually regulated by Otx2. We isolated a full-length cDNA and found that *Pikachurin* encodes a 1,017 amino acid protein that contains an N-terminal signal sequence, two fibronectin 3 (FN3), three laminin G and two EGF-like domains (**Fig. 1a** and **Supplementary Fig. 1**). We found that pikachurin was highly conserved in vertebrates, as indicated by the sequence similarity between mouse and zebrafish in the N-terminal FN3-containing domain (57%) and in the C-terminal laminin G repeats (84%) (**Fig. 1a** and **Supplementary Fig. 1**). The C-terminal half of pikachurin showed substantial similarity with agrin and perlecan (**Fig. 1b**).

Pikachurin is expressed in developing photoreceptors

To examine the tissue specificity of *Pikachurin* expression, we carried out a northern blot analysis with adult mouse tissues. We observed a single, strong 4.7-kb band in the mouse retina and faint bands in the lung and ovary (**Fig. 1c**). Although the *Pikachurin* transcript was not detected in the brain by northern blot analysis, we observed a faint *Pikachurin* band by RT-PCR analysis (**Supplementary Fig. 1**). We also detected *Pikachurin* expression in the pineal gland by RT-PCR but not in the inner ear at adult stage (**Supplementary Fig. 1**).

Furthermore, we carried out *in situ* hybridization using developing and adult mouse eye sections (**Fig. 1d–g**). *Pikachurin* expression was first detected at embryonic day 14.5 (E14.5) in the outer part of the neuroblastic layer (NBL), corresponding to the prospective photoreceptor layer (**Fig. 1d**). At this stage, cone genesis has reached its peak period and rod generation has been initiated[21]. At E17.5, a steady signal was observed (**Fig. 1e**). During postnatal retinal development, *Pikachurin* expression was observed in the photoreceptor layer (**Fig. 1f**) at postnatal day 6 (P6). This decrease in pikachurin expression in the later stages of photoreceptor development was confirmed by northern blotting (**Supplementary Fig. 1**). The expression level of pikachurin peaked at P6 and then decreased after this time point; however, a detectable level of pikachurin expression was maintained in the adult retina (**Fig. 1g**).

Pikachurin localizes in the vicinity of synaptic ribbon

To investigate the localization of pikachurin protein, we raised an antibody to pikachurin. We immunostained sections of adult mouse retina using this antibody. In the adult retina, pikachurin specifically localized to the OPL (**Fig. 2a**) in a punctate pattern (**Fig. 2b**). In

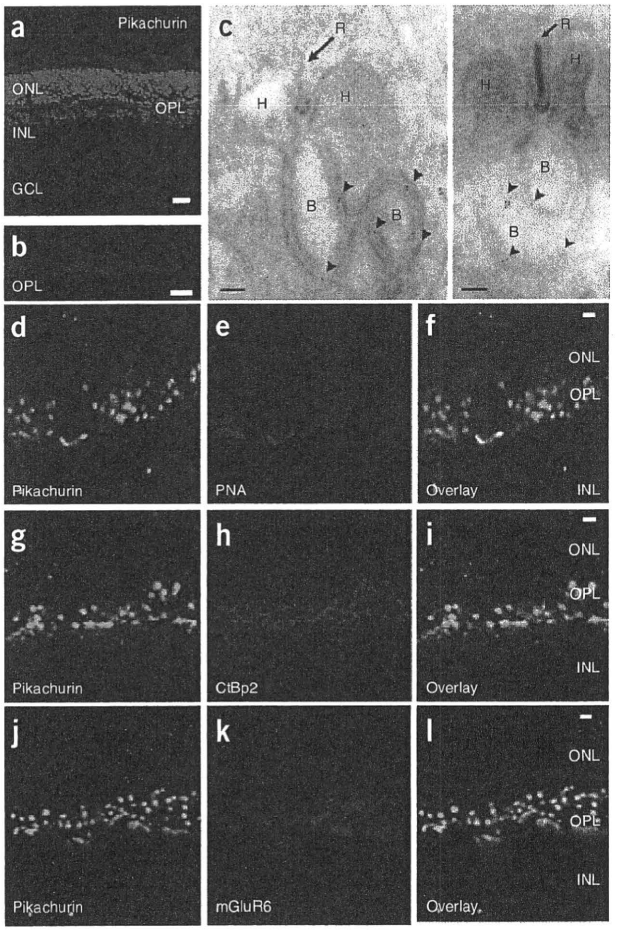

Figure 2 Pikachurin localizes to the synaptic cleft of photoreceptor ribbon synapse in the OPL. (**a**,**b**) Immunostaining of 6-month-old wild-type retina using antibody to pikachurin (red) with DAPI (blue) (**a**), which stains nuclei, or without DAPI at a higher magnification (**b**). Pikachurin localized to the OPL in the adult mouse retina in punctated pattern. Scale bars represent 20 μm in **a** and 10 μm in **b**. (**c**) Ultrastructural analysis of pikachurin localization in the ribbon synapse by electron microscopic immunocytochemistry. The pikachurin signals were localized to the synaptic cleft in the rod spherule (arrow heads). B and H indicate synaptic terminals of bipolar and horizontal cells, respectively. R indicates a synaptic ribbon. Scale bar represents 100 nm. (**d–f**) Confocal images of OPLs that were double-labeled with antibody to pikachurin (green) and PNA (red), a marker for cone pedicles of synaptic terminals, showing that pikachurin was colocalized with cone synaptic terminus. (**g–i**) Pikachurin-positive (green) puncta were localized to the INL side of horseshoe-like structures of synaptic ribbons that stained with CtBp2 (red), indicating that pikachurin is juxtaposed to, but not overlapping with, the synaptic ribbon structure. (**j–l**) Pikachurin (green) signal was observed at the photoreceptor side of mGluR6 staining (red), which is restricted to the postsynaptic site of the ON bipolar cells in the ribbon synapse of OPL. GCL, ganglion cell layer; INL, inner nuclear layer; ONL, outer nuclear layer, OPL, outer plexiform layer. Scale bars represent 20 μm in **d–l**.

contrast, no pikachurin signal was detected in the inner plexiform layer (IPL), where ribbon synapses are formed between bipolar cells and either ganglion or amacrine cells (data not shown).

To investigate more precisely the localization of pikachurin in the OPL, we carried out electron microscopic immunocytochemistry using our antibody to pikachurin. As shown in **Figure 2c**, the terminus of rod photoreceptors usually contains a single large ribbon that bends around four deeply invaginating postsynaptic elements, the dendrites of bipolar cells and processes of horizontal cells[3]. The pikachurin signals were mainly observed in the synaptic cleft around the bipolar cell dendritic tips in the rod spherule (**Fig. 2c**).

To examine whether pikachurin localizes to the cone pedicle, we immunostained the retina using our antibody to pikachurin and rhodamine-labeled peanut agglutinin (PNA), which specifically binds to glycolipids on the surface of cone pedicles[22]. PNA signals overlapped with those of pikachurin, indicating that pikachurin localized to cone synaptic terminals as well as to rod synaptic terminals (**Fig. 2d–f**).

Next, we analyzed the localization of pikachurin by staining with the synaptic ribbon markers bassoon and CtBp2/RIBEYE. Bassoon is a presynaptic cytomatrix protein that is essential for photoreceptor ribbon synapse formation and localizes to the base of the photoreceptor synaptic ribbon, a site of neurotransmitter release[23]. CtBp2/RIBEYE is a specific component of synaptic ribbons in the OPL and IPL of the retina[24]. We observed that pikachurin localized in the ribbon synapses to the inner nuclear–layer side of horseshoe-like structures of synaptic ribbons stained with bassoon (data not shown) and CtBp2/RIBEYE (**Fig. 2g–i**).

The localization of metabotropic glutamate receptor subtype 6 (mGluR6) is restricted to the postsynaptic site of ON bipolar cells in the ribbon synapses of the OPL[25]. We observed the pikachurin signal at the photoreceptor side of mGluR6 staining with a small partial overlap (**Fig. 2j–l**). These results suggest that pikachurin localizes to the synaptic cleft of the ribbon synapse primarily around the postsynaptic terminals of bipolar cells.

Pikachurin is required for apposition of bipolar dendrite

To investigate a possible role for *Pikachurin* in ribbon synapse formation and/or maintenance of the retina, we generated *Pikachurin* null mice by targeted gene disruption. We deleted the first exon, which contains a start codon, of the pikachurin open reading frame (**Fig. 3a**). We confirmed the deletion in the genomic DNA of the *Pikachurin* null mouse by Southern blot (**Fig. 3b**). Total RNAs from the adult retina were analyzed by northern blots using 5′ and 3′ fragments of mouse *Pikachurin* cDNA as probes. No substantial *Pikachurin* transcript or protein was detected in *Pikachurin* null mouse retinas (**Fig. 3c,d** and **Supplementary Fig. 2** online).

Pikachurin$^{-/-}$ mice were born in Mendelian ratios (data not shown). Both *Pikachurin*$^{+/-}$ and *Pikachurin*$^{-/-}$ mice showed no gross morphological abnormalities, and were viable and fertile under normal conditions in the animal facility. Histological examination revealed no obvious differences among wild-type, *Pikachurin*$^{+/-}$ and *Pikachurin*$^{-/-}$ mouse retinas at 6 months (**Fig. 3e–m** and **Supplementary Fig. 3** online).

To examine ultrastructural differences between wild-type and *Pikachurin*$^{-/-}$ mouse retinas, we carried out a conventional electron microscopy analysis. Although we did not find any substantial difference in the photoreceptor outer segments and ribbon synapses in the IPL (data not shown), we observed an absence of the tips of the bipolar cell dendrites in the *Pikachurin*$^{-/-}$ rod ribbon synapses (**Fig. 4a–d**) as well as those of cone photoreceptors (**Supplementary Fig. 4** online). To further examine this result, we analyzed the photoreceptor synaptic terminals of the wild-type and *Pikachurin*$^{-/-}$ retinas quantitatively (**Fig. 4e**). We prepared ultrathin sections from adult (3 month old) wild-type and *Pikachurin*$^{-/-}$ mouse retinas and randomly photographed them. For the quantitative analysis, we focused on rod photoreceptors, as they comprise ~99% of the photoreceptors in the

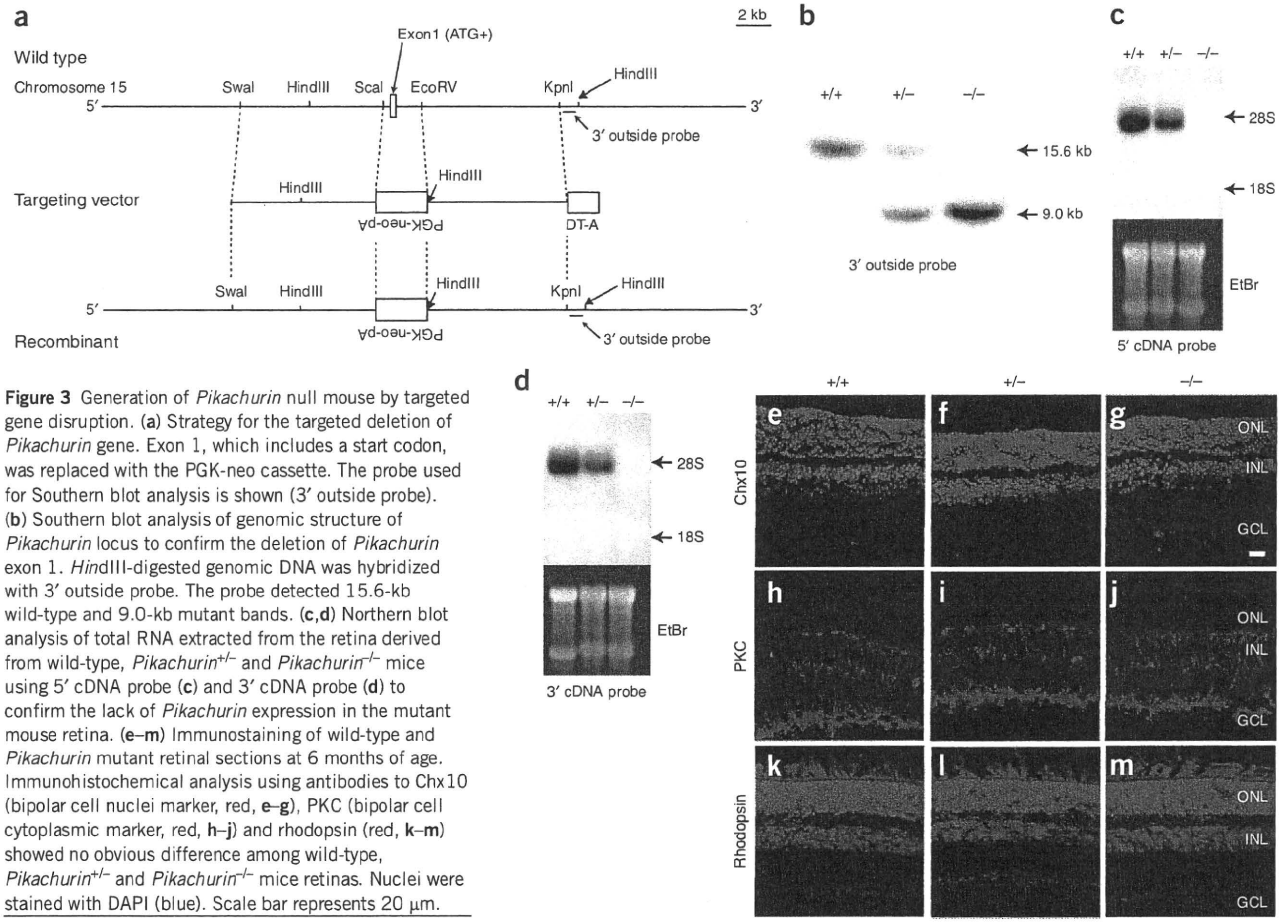

Figure 3 Generation of *Pikachurin* null mouse by targeted gene disruption. (**a**) Strategy for the targeted deletion of *Pikachurin* gene. Exon 1, which includes a start codon, was replaced with the PGK-neo cassette. The probe used for Southern blot analysis is shown (3′ outside probe). (**b**) Southern blot analysis of genomic structure of *Pikachurin* locus to confirm the deletion of *Pikachurin* exon 1. *Hin*dIII-digested genomic DNA was hybridized with 3′ outside probe. The probe detected 15.6-kb wild-type and 9.0-kb mutant bands. (**c**,**d**) Northern blot analysis of total RNA extracted from the retina derived from wild-type, *Pikachurin*$^{+/-}$ and *Pikachurin*$^{-/-}$ mice using 5′ cDNA probe (**c**) and 3′ cDNA probe (**d**) to confirm the lack of *Pikachurin* expression in the mutant mouse retina. (**e**–**m**) Immunostaining of wild-type and *Pikachurin* mutant retinal sections at 6 months of age. Immunohistochemical analysis using antibodies to Chx10 (bipolar cell nuclei marker, red, **e**–**g**), PKC (bipolar cell cytoplasmic marker, red, **h**–**j**) and rhodopsin (red, **k**–**m**) showed no obvious difference among wild-type, *Pikachurin*$^{+/-}$ and *Pikachurin*$^{-/-}$ mice retinas. Nuclei were stained with DAPI (blue). Scale bar represents 20 μm.

mouse retina[23]. A normal rod synaptic terminus contains a single ribbon synaptic site, where glutamate is released onto the postsynaptic elements, horizontal cell processes and rod bipolar cell dendrites. The postsynaptic elements invaginate into the rod terminal and form a triadic or tetradic configuration adjacent to the ribbon site (**Fig. 4a** and **Supplementary Fig. 5** online)[23,26]. In the adult *Pikachurin*$^{-/-}$ retina, we observed rod terminals containing invaginated bipolar terminals in only 3% of the sections, whereas we detected bipolar terminals in 53% of the wild-type retina (χ^2 test; $P < 0.001$; **Fig. 4e**). We used ultrathin sections; the vertical alignment of the sections was confirmed using photoreceptor outer segments as markers (**Fig. 4c,d**). We also found that the morphology of rod synaptic terminals varied widely even in the wild-type retina. Therefore, to confirm the precise structure of abnormal ribbon synapses in the adult *Pikachurin*$^{-/-}$ retina, we carried out electron tomography by ultrahigh-voltage electron microscopy (**Fig. 4f–k** and **Supplementary Movies 1–6**). We collected images from −60° to +60° at 2° intervals around a single axis from adult (3 month old) wild-type and *Pikachurin*$^{-/-}$ mouse retinas. The electron tomography indicates that in the terminals of bipolar cells do not appose to the synaptic terminals in the rod photoreceptor ribbon synapses the adult *Pikachurin*$^{-/-}$ retina (**Fig. 4j,k**).

We observed that the bipolar dendritic tips did not enter the invaginations in photoreceptor synaptic terminals in the *Pikachurin*$^{-/-}$ mice, but where do they end up? To address this question, we co-immunostained ribbon synapses using several synaptic markers. In the *Pikachurin*$^{-/-}$ mice, the bipolar cells, stained with protein kinase C (PKC; **Fig. 4l,m**), developed dendrites to the outer plexiform layer as well as they did in the wild type. mGluR6 accumulated at the tip of bipolar cell dendrites in both the wild-type and *Pikachurin*$^{-/-}$ mouse retina (**Fig. 4l,m**). CtBP2 was observed in the vicinity of the tips of bipolar dendrites in both the wild-type and *Pikachurin*$^{-/-}$ retina (**Fig. 4n,o**). A similar distribution of cone synaptic marker, PNA, was also observed in cone photoreceptor terminals (**Fig. 4p,q**). These data suggest that the bipolar dendritic terminals remain in close vicinity to photoreceptor terminals and seem to retain at least some integrity for the connection between photoreceptors and bipolar cells, even in the *Pikachurin*$^{-/-}$ retina.

Pikachurin is required for synaptic signal transmission

To evaluate the physiological function of *Pikachurin in vivo*, we measured ERGs on 2-month-old wild-type and *Pikachurin*$^{-/-}$ mice (**Fig. 5a–f**). The scotopic ERGs elicited by different stimulus intensities from a wild-type and a *Pikachurin*$^{-/-}$ mice are shown in **Figure 5a**. In the wild-type mouse, only a positive b-wave, which originates from the rod bipolar cells[27], was seen at lower stimulus intensities (−5.0 to −3.0 log cd s m^{-2}). At higher stimulus intensities (−1.0 to 1.0 log cd s m^{-2}), the negative a-wave, which originates mainly from the activity of the rod photoreceptors, appeared. The amplitude and implicit time of the a-wave of the dark-adapted ERGs were nearly the same for both types of mice, indicating that the rod photoreceptors are functioning normally in *Pikachurin*$^{-/-}$ mice (**Fig. 5a**). In contrast, the amplitude of the dark-adapted ERG b-wave in *Pikachurin*$^{-/-}$ mice

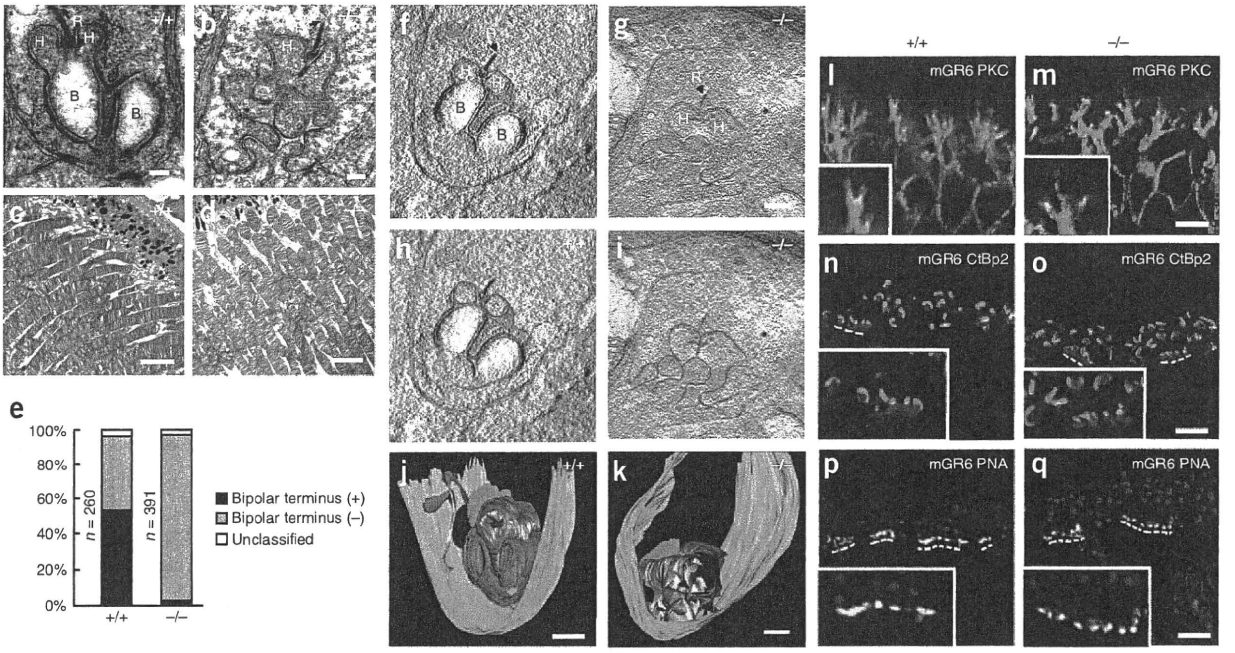

Figure 4 Pikachurin is required for proper apposition of bipolar dendritic tips to the photoreceptor synaptic terminus. (**a–d**) Ultrastructural analysis of ribbon synapses (**a**,**b**) and outer segments (**c**,**d**) in wild-type (**a**,**c**) and *Pikachurin*$^{-/-}$ (**b**,**d**) mouse retinas. Synaptic ribbon (R), horizontal cell processes (H) and bipolar cell dendrites (B) are shown. Scale bars represent 200 nm in **a** and **b** and 5 μm in **c** and **d**. (**e**) Quantitative analysis of defective bipolar cell dendrites in the wild-type (+/+) and *Pikachurin*$^{-/-}$ mouse retina. (**f–k**) Electron tomography of rod photoreceptor synapse terminals using ultrahigh-voltage electron microscopy. Representative images of retinal sections derived from wild-type (**f**,**h**,**j**) and *Pikachurin*$^{-/-}$ retinas (**g**,**i**,**k**). Representative demarcation of bipolar dendritic tips (magenta), horizontal processes (dark blue), ribbon (green) and rod plasma membrane (light blue) for tomography are shown for wild-type (**h**) and *Pikachurin*$^{-/-}$ (i) retinas (see **Supplementary Movies 1–6**). Scale bar = 300 nm. (**l–q**) Bipolar cell dendrites ended in the vicinity of photoreceptor terminals in *Pikachurin*$^{-/-}$ retina. mGluR6 (red) localized to the tip of bipolar cell dendrites stained with antibody to PKC (green) both in wild-type (**l**) and *Pikachurin*$^{-/-}$ retinas (**m**). The tips of bipolar cell dendrites stained with antibody to mGluR6 (red) localized in the vicinity of photoreceptor synaptic ribbons (green) both in the wild-type (**n**) and *Pikachurin*$^{-/-}$ retinas (**o**). Clustered cone synaptic terminals (broken lines) stained with PNA (green) colocalized with the tips of bipolar cell dendrites (red) in the wild-type (**p**) and the *Pikachurin*$^{-/-}$ (**q**) retinas.

was reduced at lower stimulus intensities of −5.0 to −3.0 log cd s m^{-2} but approached the normal range at higher stimulus intensities of −1.0 to 1.0 log cd s m^{-2} (**Fig. 5b**).

The most notable finding in this mutant mouse was the delay in the scotopic ERG b-wave (**Fig. 5c**). The implicit times of the scotopic ERG b-wave were severely delayed at all stimulus intensities, and the delay was more than 100 ms at the highest intensities. These results suggest that the signal transmission from the rod photoreceptors to the rod bipolar cells is less sensitive and is delayed in this mutant mouse.

To determine whether the abnormality in the signal transmission from the photoreceptors to the bipolar cells exists in the cone pathway, we recorded photopic ERGs from both types of mice (**Fig. 5d**). The amplitude of the a-wave of the photopic ERGs in *Pikachurin*$^{-/-}$ mouse was relatively larger than that of wild-type mouse, which was a result of the delay and reduction of the positive b-wave (**Fig. 5d**). The amplitude of the b-wave of the photopic ERGs was reduced and the implicit times were delayed at all stimulus intensities (**Fig. 5e,f**). These results indicate that the signal transmission from cone photoreceptors to the cone bipolar cells was also impaired in the *Pikachurin*$^{-/-}$ mouse.

We also recorded the collicular visual-evoked potentials (VEPs) in the *Pikachurin*$^{-/-}$ mouse. We did not observe any differences in the VEPs of wild-type and *Pikachurin*$^{-/-}$ mice in both scotopic and photopic conditions (**Fig. 5g,h**). This result suggests that VEPs may not be sensitive enough to reflect the ERG b-wave delay that we observed in the mutant retina and that the visual transmission pathway in the brain is not affected in *Pikachurin*$^{-/-}$ mice. We then investigated the optokinetic responses (OKRs) of 3-month-old wild-type and *Pikachurin*$^{-/-}$ mice induced by rotation of a screen with various spatial frequencies of black and white stripes (**Fig. 5i–k**). The *Pikachurin*$^{-/-}$ mouse showed similar OKRs by rotation of screens with 15- and 1.92-deg frequencies (gain was close to 1.0; **Fig. 5j,k**); however, its OKR at the 1.25-deg screen was significantly weaker than that of wild-type mice (unpaired *t* test, $P < 0.01$; **Fig. 5j,k**). Rotation of the 0.91-deg screen did not show significant OKR difference in either line ($P = 0.20$; **Fig. 5j,k**). Thus, *Pikachurin*$^{-/-}$ mice did not show noticeable impairment with relatively large angle stripes, but their sensitivity to small angle stripes was significantly impaired.

Pikachurin is a physiological ligand of α-dystroglycan

Many individuals with Duchenne muscular dystrophy (DMD) and Becker muscular dystrophy (BMD) have been known to show an abnormal dark-adapted ERG b-wave[17,28,29]. In mice, previous reports showed that certain dystrophin-disrupted alleles (*mdx*^{Cv2} and *mdx*^{Cv4}, alleles of *Dmd*) caused prolongation of the implicit time of the b-wave[18]. Functional defects of α-dystroglycan in *Large*-deficient mice (*Large*^{myd} and *Large*^{vls}) also produce a similar ERG phenotype to *Pikachurin* null mice[30]. In addition, agrin, perlecan and several laminin α-isoforms can all interact with α-dystroglycan by a laminin G domain–dependent mechanism[9]. These observations suggest that there is a possible functional interaction between dystroglycan and pikachurin. To investigate this issue, we first examined the localization of pikachurin, dystroglycan and dystrophin by co-immunostaining in

the retina (**Fig. 6a–f**). At 6 months, pikachurin stained in a grainy pattern in the OPL of the retina (**Fig. 6a,d**). Notably, both β-dystroglycan and dystrophin were expressed in a similar grainy pattern, overlapping with pikachurin signals (**Fig. 6b,c,e,f**).

As shown above (**Fig. 1a,b**), structural anticipation suggests that pikachurin LG domains have similarity with LG domains of agrin and perlecan. Because both proteins are known to bind to α-dystroglycan via their LG domains[10,31], we investigated whether pikachurin LG domains bind to α-dystroglycan. To test this binding, we prepared recombinant pikachurin LG domains (residues 391–1,017) as a His-tag protein (pikachurin-LG–His) and recombinant α-dystroglycan as an Fc-fusion protein (DG-Fc). Pikachurin-LG–His was recovered in the NP-40–solubilized cell lysate. DG-Fc and its control Fc proteins were secreted into the cell culture media when expressed in NIH 3T3 cells. We confirmed that DG-Fc was recognized by a monoclonal antibody (IIH6) against glycosylated forms of α-dystroglycan (data not shown). We prepared DG-Fc–protein A beads, which were then mixed with the cell lysate that contained pikachurin-LG–His. The binding reaction was carried out in the presence of Ca^{2+} and Mg^{2+} or EDTA, as binding between α-dystroglycan and agrin or perlecan requires divalent cations[10,32,33]. Western blotting analysis of the bound materials using antibody to His revealed that the pikachurin LG domains bind to DG-Fc (**Fig. 6g**). This binding was inhibited by EDTA (**Fig. 6g**), which indicates that there is a divalent cation-dependent interaction, as is the case of laminin, agrin and perlecan[31]. We confirmed that pikachurin-LG–His did not bind to the Fc protein (**Fig. 6g**). In addition, the inhibitory effects of IIH6 (**Fig. 6h**) suggest that the pikachurin binding to α-dystroglycan is glycosylation-dependent, as IIH6 is reported to inhibit binding of laminin and perlecan[33,34]. Both

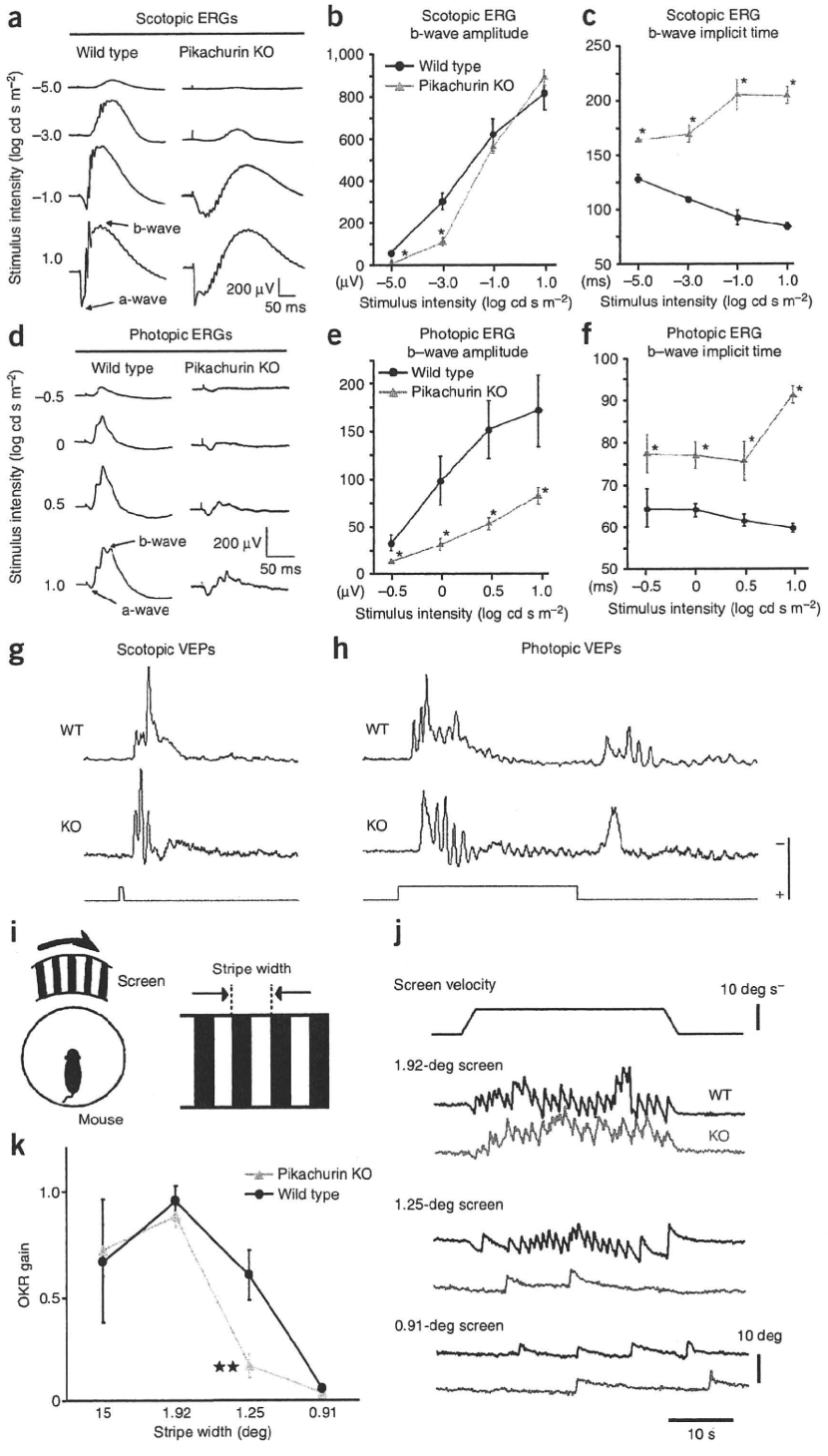

Figure 5 Electrophysiological and OKR analyses of wild-type and *Pikachurin* null mice. (**a–f**) ERG analysis of *Pikachurin*$^{-/-}$ mice. Scotopic (**a**) and photopic (**d**) ERGs were elicited by four different stimulus intensities from both wild-type and *Pikachurin*$^{-/-}$ (KO) mice ($n = 4$). Amplitude (**b**) and implicit time (**c**) of scotopic ERG b-waves as a function of the stimulus intensity are shown. Amplitude (**e**) and implicit time (**f**) of photopic ERG b-waves are shown. The bars indicate s.e.m. Asterisks indicate that the differences are statistically significant (Mann-Whitney test, $P < 0.05$). (**g,h**) VEPs in the superior colliculus of wild-type (WT) and *Pikachurin*$^{-/-}$ (KO) mice. (**g**) Under scotopic conditions, a brief 10-ms stimulation was applied from the LED panel (238 cd m^{-2}) in the front of the left eye. (**h**) Under photopic condition, a 500-ms stimulation was applied to examine both ON and OFF responses. The bottom trace indicates the onset and offset of a light stimulus. Scale bar indicates 200 μV. (**i–k**) OKR analysis of wild-type and *Pikachurin*$^{-/-}$ mice. A schematic drawing of OKR recording (**i**). (**j**) Screen velocity, scale bar represents 10° s^{-1}. Examples of OKRs in wild-type (black) and *Pikachurin*$^{-/-}$ (gray) mice with a 1.92-, 1.25- or 0.91-deg screen. (**k**) OKR gain with four screens of different stripe width. Bar indicates s.d. (gray triangle, *Pikachurin*$^{-/-}$ mice; black circle, wild-type mice, $n = 6$). OKR of *Pikachurin*$^{-/-}$ mice with 1.25-deg screen was significantly weaker than that of wild-type mice (unpaired *t* test, $P < 0.01$).

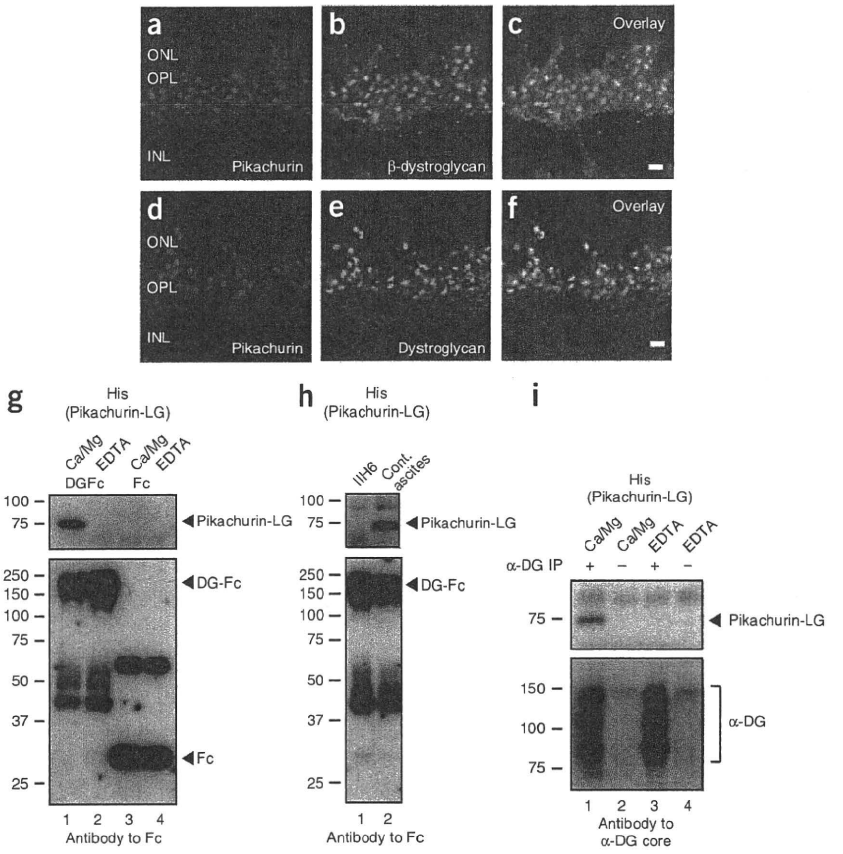

Figure 6 Interaction and colocalization of pikachurin with dystroglycan. (**a–f**) Confocal images of OPLs that were double labeled with antibodies to pikachurin (red, **a**,**d**) and β-dystroglycan (green, **b**) or dystrophin (green, **e**), showing that pikachurin colocalized with DGC molecules (**c**,**f**). Scale bars represent 2 μm. (**g**) Molecular interaction between pikachurin and α-dystroglycan. DG-Fc (lanes 1 and 2) or Fc (lanes 3 and 4) proteins were coupled with protein A beads and incubated with cell lysates containing pikachurin-LG–His in the presence of Ca^{2+} and Mg^{2+} (lanes 1 and 3) or EDTA (lanes 2 and 4). Bound materials were analyzed by western blotting with antibody to His tag (upper). A comparable amount of DG-Fc or Fc proteins on protein A beads were confirmed by staining with an antibody to Fc (lower). (**h**) Inhibitory effect of IIH6 on the interaction between pikachurin and α-dystroglycan. The binding reaction was carried out with (lane 1) or without (lane 2) the monoclonal antibody to α-dystroglycan IIH6. IIH6 selectively recognized glycosylated forms of α-dystroglycan. (**i**) Pikachurin interaction with eye α-dystroglycan. Native α-dystroglycan was immunoprecipitated from mouse eye extracts with antibody to α-DG core protein (lanes 1 and 3). For negative controls, antibody to α-DG core protein was omitted (lanes 2 and 4). The eye α-DG–protein G beads were tested for pikachurin binding in the presence of Ca^{2+} and Mg^{2+} (lanes 1 and 2) or EDTA (lanes 3 and 4). The samples were analyzed by western blotting with antibodies to His tag and α-DG core.

laminin and perlecan require α-dystroglycan glycosylation, which is recognized by IIH6, for binding to α-dystroglycan[35]. These data provide evidence of a direct interaction between pikachurin and α-dystroglycan.

To confirm the physiological interaction between pikachurin and α-dystroglycan in the retina, we carried out a pull-down assay using dystroglycan purified from murine retina. α-dystroglycan was immunoprecipitated from an eye extract using a specific antibody and assayed for an interaction with pikachurin. Consistent with our results using the recombinant α-dystroglycan, α-dystroglycan purified from murine eye interacts with pikachurin in a divalent cation–dependent manner (**Fig. 6i**). Furthermore, immunofluorescence analysis showed colocalization of pikachurin with both dystroglycan and dystrophin in the OPL (**Fig. 6a–f**), suggesting that pikachurin is a physiological ligand of α-dystroglycan in the retina.

DISCUSSION

Functional roles of *Pikachurin* in ribbon synapse formation

Structurally, synapses are specialized sites of cell-cell contact. Cell adhesion molecules and ECM proteins have been suspected, and in some cases have been demonstrated, to be important in synapse development and plasticity. In *Drosophila*, N-cadherins on both photoreceptor cells and their target neurons in the optic neuropil are required for proper target selection[36]. In vertebrates, however, cadherins do not seem to function in target recognition[37]. Agrin, an ECM molecule, has been extensively studied and proven to be required for postsynaptic differentiation, especially clustering of acetylcholine receptors, of the neuromuscular junction (NMJ)[38]. However, the effect and function of these cell adhesion and ECM molecules in synapse formation in the vertebrate CNS remain poorly understood. In the current study, our results demonstrate that a previously unknown ECM-like protein, pikachurin, is essential for proper bipolar dendritic tip apposition to the photoreceptor ribbon synapse. Notably, in the *Pikachurin* null retina, the tips of the bipolar cell dendrites are absent in photoreceptor ribbon synapse, but the horizontal cell terminus is not substantially affected. Immunostaining with antibody to mGluR6 or PKC in *Pikachurin* null retina did not show substantial differences in bipolar morphology (**Fig. 4l,m**), suggesting that bipolar cell differentiation is not perturbed. ERG studies showed that synaptic signal transmission from photoreceptors to bipolars was substantially prolonged but not lost. This suggests that the tips of the bipolar cell dendrites do not enter the invagination of photoreceptor terminals but still exist some distance apart from the ribbon synapse. This phenotype may be due to supporting molecules involved in photoreceptor-bipolar interaction, although pikachurin has a major role. Does the absence of the bipolar cell dendrite tips in the photoreceptor synapse occur because of a developmental defect or a maintenance abnormality after a normal synapse develops? Dynamic *Pikachurin* expression in developing photoreceptors (**Fig. 1d–g** and **Supplementary Fig. 1**) suggests that this phenotype is the result of developmental defects.

In this study, we focused our analysis on rod photoreceptor synapses (**Fig. 4a–k**), as the very small number of cones makes analysis with enough numbers of samples extremely difficult. However, several micrographs of cone synaptic terminals (**Supplementary Fig. 4**) and ERG results (**Fig. 5d–f**) suggest that similar synaptic abnormality probably occurs in cone photoreceptor synapses as was observed in rods. Typical ribbon synapses also exist in bipolar cell terminals in